Available online at www.sciencedirect.com
ScienceDirect
Journal of the European Ceramic Society 30 (2010) 1139–1144
www.elsevier.com/locate/jeurceramsoc

Electrophoretic deposition (EPD) of WO_3 nanorods for electrochromic application

Eugene Khoo, Pooi See Lee, Jan Ma *

School of Materials Science and Engineering, Nanyang Technological University, Singapore 639798, Singapore

Available online 10 June 2009

Abstract

Electrophoretic deposition (EPD) was applied in coating hydrothermally synthesized crystalline tungsten oxide (WO_3) nanorods onto ITO glass for electrochromic application. Nanorods suspension of 10 mg/cm^3 was used in the EPD with optimum electric field of 5–6 V/cm. Saturation in WO_3 deposited amount at electric field >7 V/cm was observed during constant voltage EPD. This could be attributed to the oxide layer shielding effect on the electric field induced electrophoresis. Constant current EPD from 0.2 mA/cm^2 to 1.4 mA/cm^2 was also performed for the WO_3 nanorods. The deposited amount of nanorods was found to be proportional to the current density from 0.2 mA/cm^2 to 0.8 mA/cm^2 under constant deposition duration. However, the deposited amount decreased at current density >0.8 mA/cm^2. This could be due to the high deposition rate that resulted in poor adhesion and hence nanorods peel off during the substrate removal. It was noted that the EPD of nanorods followed a linear relationship in I vs. $t^{-1/2}$ plot according to Cottrell equation, which implied that the reaction was a diffusion controlled process. The EPD coated substrate was tested in 1 M $LiClO_4$/propylene carbonate (PC) electrolyte for electrochromic studies. The porous WO_3 nanorods layer exhibited optical modulation $\Delta T_{700\,nm}$ of 40%, moderate coloration time $t_c^{70\%}$ of 28.8 s and improved bleaching time $t_b^{70\%}$ of 4.5 s, which could be due to the porous oxide layer with large surface area that facilitates the ion insertion/extraction and the electrolyte penetration in the oxide layer shortens the ionic diffusion length of Li.

Keywords: Transition metal oxides WO_3; Optical properties; Suspensions; Functional applications; Electrochromic

1. Introduction

Tungsten oxide (WO_3) is one of the widely studied transition metal oxides for its attractive application such as energy efficient windows (smart windows), antiglare automobile rear-view mirrors, sunroofs and sensors.[1–5] WO_3 has the optical modulation between transparent and blue color upon the ion-electron double injection, which is known as electrochromism. The reaction can be expressed as

$$WO_3(\text{transparent}) + xe^- + xM^+ \Leftrightarrow M_xWO_3(\text{blue}) \quad (1)$$

where M^+ stands for the cations such as H^+, Li^+ Na^+ or K^+.

Various methods such as sol–gel,[6] electrodeposition,[7] hydrothermal process,[8] evaporation[9] and sputtering[10] have been applied in the formation of crystalline and amorphous WO_3. Among these methods, hydrothermal process has received huge attention for its advantages such as simple operation, low-cost, potential for large scale production and forming crystalline structure with good stability.[11] However, one of the process drawbacks is that the hydrothermally synthesized products are dispersed as a suspension and additional assembly steps are required to adhere the dispersed products onto the substrate. Electrophoretic deposition (EPD), on the other hand, is an attractive process where the charged particles or nanostructures in a suspension can be driven onto the electrode surface under the influence of an electric field. This method is efficient in forming a film or coating on conductive surface (even a complex surface morphology) with the control in film thickness and porosity through the electric field, pH value and deposition duration. EPD has provided flexibilities in designing electrochromic devices with different degrees of optical modulation (film thickness) and switching time (film porosity) and hence widen their application in advanced technologies.

EPD has been applied in surface coating, ceramics processing and forming composite materials[12–14] where particles are usually used as the starting material in the deposition. Recently, Girishkumar et al.[15] and Boccaccini et al.[16] have reported the 1D nanostructure EPD of CNT and Yu and Zhou[17] have success-

* Corresponding author. Tel.: +65 67906214; fax: +65 67909081.
E-mail address: asjma@ntu.edu.sg (J. Ma).

0955-2219/$ – see front matter © 2009 Elsevier Ltd. All rights reserved.
doi:10.1016/j.jeurceramsoc.2009.05.014

fully demonstrated the EPD of titanate nanotubes with diameter around 10 nm. These results suggest that the EPD is also applicable in 1D nanostructures assembly. In this work, WO_3 1D nanorods constant voltage and constant current EPD were performed on a transparent conductive substrate (ITO glass). Optimum deposition conditions were identified with a discussion in the deposition mechanism. The resultant electrochromic performances such as optical modulation and switching time of the WO_3 nanorods coated substrates were also studied.

2. Experimental details

2.1. WO_3 synthesis

Tungsten oxide (WO_3) nanorods were prepared through hydrothermal process: 0.825 g of $Na_2WO_4{\cdot}2H_2O$ (Aldrich, 99%) and 0.290 g of NaCl (Sigma Ultra, 99.5%) were dissolved in 20 ml of de-ionized water with a mole ratio of 1:2. The solution was adjusted with 3.0 M HCl until a pH of 2, then transferred into the Teflon liner of the stainless steel autoclave and heated at 180 °C for 24 h. White precipitate of nanorods was obtained and centrifuged with ethanol and de-ionized water for several times to remove any left over precursors. The WO_3 nanorod was found to be a hexagonal single crystal with a growth direction of (0 0 0 2). The diameter and length of the nanorod were around 100 nm and 2 μm, respectively.[18]

2.2. Electrophoretic deposition (EPD)

The nanorods suspension was prepared by dispersing the WO_3 nanorods in de-ionized water with 10 mg/cm^3 concentration, −40 mV zeta potential and a pH value around 6.77. Transparent conductive substrate – ITO coated glass (Delta Technologies, Rs = 15–25 Ω) was used as the working electrode in order to study the electrochromic performances of the WO_3 nanorods while a Pt wire was used as the counter electrode. The working electrode (ITO glass) was kept at positive voltage or current with distance between the two electrodes remained as 1 cm. The deposition was carried out by Autolab Potentiostat (PGSTAT302) with a maximum voltage limit of 10 V. Constant voltage and current EPD were carried out with an electric field ranged from 3 V/cm to 8 V/cm and current density ranged from 0.2 mA/cm^2 to 1.4 mA/cm^2, respectively. The current and voltage responses were recorded with respect to the deposition duration for further analysis. The coated substrates were overnight air-dried before morphology and electrochromic studies. Surface morphology of the coated ITO was characterized using field emission scanning electron microscopy (FESEM, JOEL6340F) and the oxide layer thickness was checked by Alpha-step Surface Profiler.

2.3. Electrochromic studies

Optical modulation and switching studies were carried out in a two-electrode system for ±3 V. The coated ITO was used as the working electrode and a Pt wire was used as the counter and reference electrode. All electrochemical studies were carried out in an electrolyte of 1.0 M $LiClO_4$ in propylene carbonate (PC). Transmittance variation and color changes were detected through UV–vis spectrometer (Shimadzu UV-2501PC) at visible wavelength ranged from 300 nm to 900 nm. Optical modulation and switching time were extracted from the transmittance spectra.

3. Results and discussion

3.1. Electrophoretic deposition (EPD)

WO_3 nanorods suspension of 10 mg/cm^3 was used in the constant voltage EPD. The applied electric field ranged from 3 V/cm to 8 V/cm for 900 s deposition and the *I–t* behaviors are recorded in Fig. 1a. With the various electric field strength studied, the EPD of WO_3 nanorods can be characterized into three regions: no deposition (<4 V/cm), uniform deposition (5–6 V/cm) and saturated deposition (>7 V/cm). For the electric field <4 V/cm, the electric field induced driving force is not strong enough to drive the WO_3 nanorods onto the ITO glass. Hence, only small amount of nanorods is observed under the FESEM (Fig. 2a). When the electric field is increased beyond 5 V/cm, uniform WO_3 nanorods deposition was is observed as a porous oxide layer on top of the ITO (Fig. 2b). However, for the electric field >7 V/cm, the deposition ceases after a period of time as showed in Fig. 1a with a sharp drop in the current density until nearly

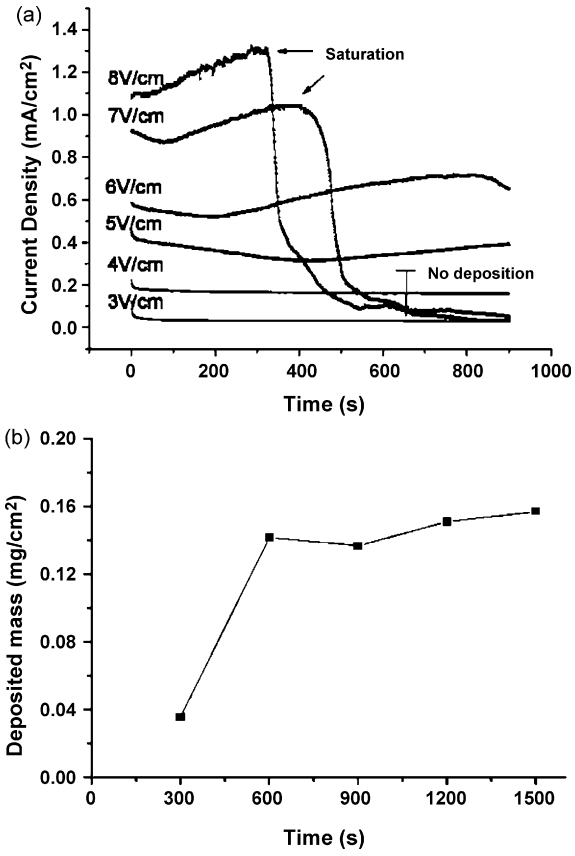

Fig. 1. (a) Constant voltage EPD of 10 mg/cm^3 WO_3 nanorods suspension for 900 s deposition and (b) WO_3 nanorods deposited amount at 5 V/cm for 300–1500 s deposition duration.

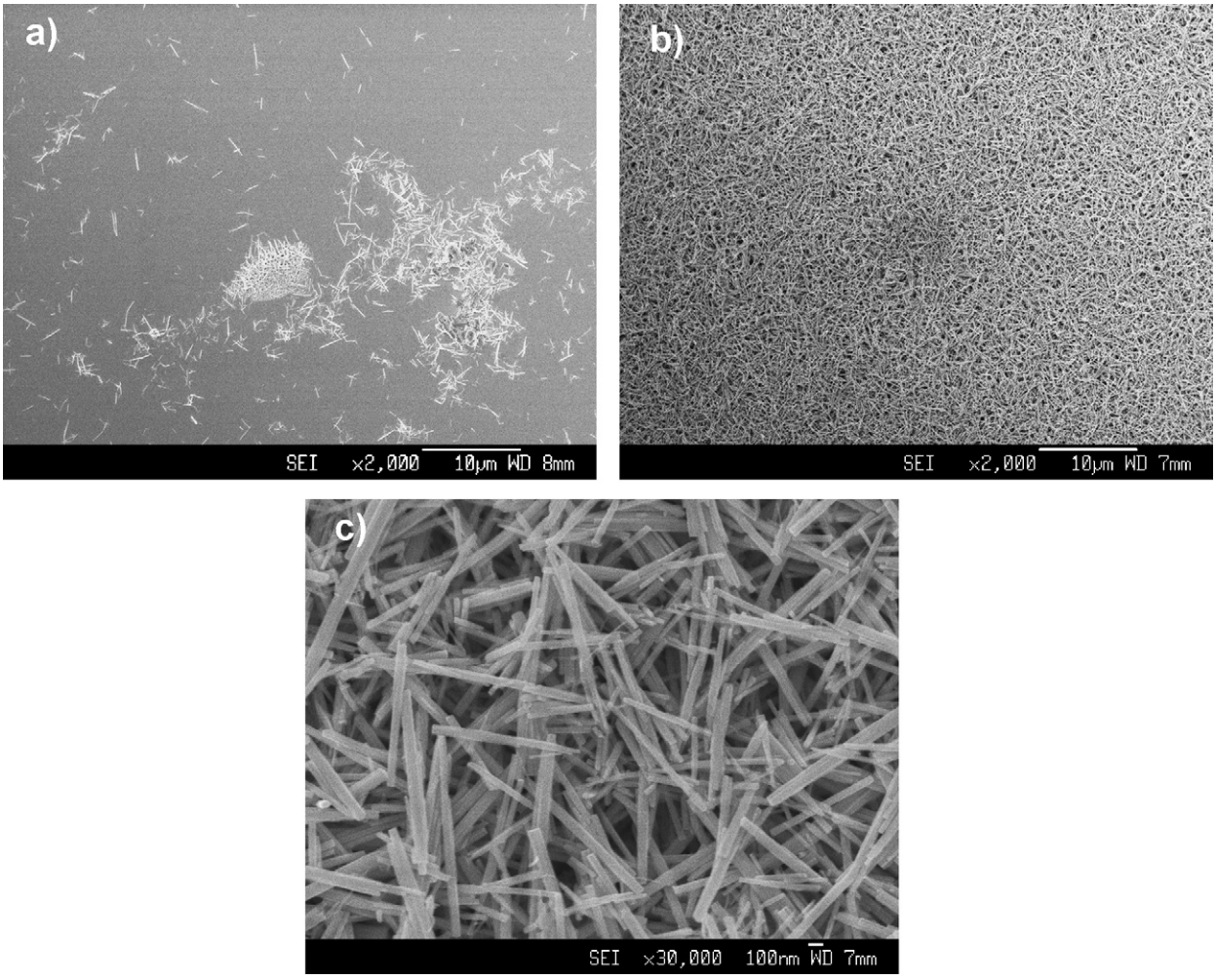

Fig. 2. FESEM images of the deposited WO_3 nanorods on ITO glass under (a) 4 V/cm and (b) 6 V/cm and (c) higher magnification of 6 V/cm deposited WO_3 nanorods.

zero. This might be due to the electrical resistance on the working electrode increases with the oxide layer thickness and hence decreases the electric field induced electrophoresis in the suspension. The oxide layer will weaken the driving force (due to the voltage drop across the oxide layer) and hence decrease the nanorods motion.[13] The nearly zero current density implies that the electric field induced driving force is not strong enough to drive the nanorods onto the electrode after the build-up of the oxide layer. In addition, oxide layer peeling was observed at 7 V/cm and higher electric field during the substrate removal, which causes non-uniform coverage on the ITO surface and is undesirable for the electrochromic application. Thus, it is noted that 5–6 V/cm gives the optimum deposition electric field for the present nanorods suspension. Fig. 1b shows the deposited amount with respect to the deposition duration under 5 V/cm. The relationship turns non-linear after 900 s with a nearly constant deposited amount, which corresponds to a thickness of 1.2 μm. This result further supports that EPD will cease after the build-up of the oxide layer and longer deposition duration does not significantly improve the deposited amount.[13,19,20]

Constant current density EPD was carried out using 0.6–1.4 mA/cm^2 (Fig. 3a). The voltage increased up to the maximum voltage of the potentiostat (10 V) after a period of deposition while optimum deposition was observed to be around 0.8 mA/cm^2. The deposited amount of WO_3 is plotted with respect to the current density (Fig. 3b). The deposited amount is found to increase with respect to the current density, which implies that the passed charges (current) are proportional to the electrophoresis deposited nanorods. However, at the higher current density (>0.8 mA/cm^2), the deposited amount is recorded to be reduced, which could be due to the ITO substrate degradation or poor adhesion of the nanorods to the substrate. ITO glass has been demonstrated as the working electrode for aqueous system EPD up to 40 V/cm[21] and 2.5 mA/cm^2 [22] and no ITO degradation was observed. Thus, ITO electrochemical degradation at high current density is not the reason for the decrease in deposited amount. Hence, the decrease of deposited mass can be attributed to the accumulation of large amount of WO_3 nanorods at the electrode within a short duration under a high driving force, which results in the formation of a very porous, inhomogeneous film with reduced adhesion at the electrode surface. As a result, peel-off was observed during the deposited substrate removal and lower deposited amount was remained on the substrate.

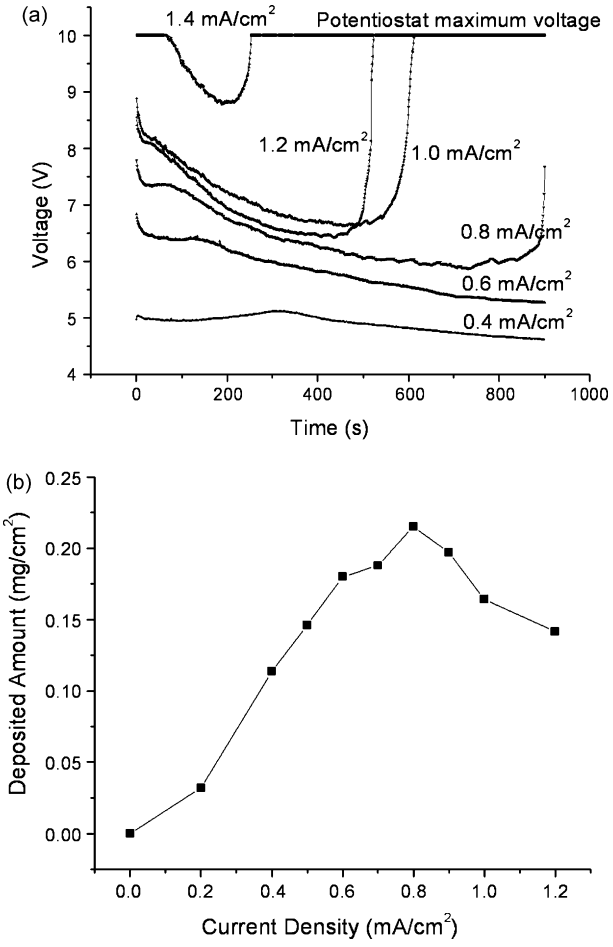

Fig. 3. (a) Constant current EPD of 10 mg/cm^3 WO_3 nanorods suspension for 900 s deposition and (b) deposited amount of WO_3 nanorods on ITO glass for 900 s deposition duration at various current densities.

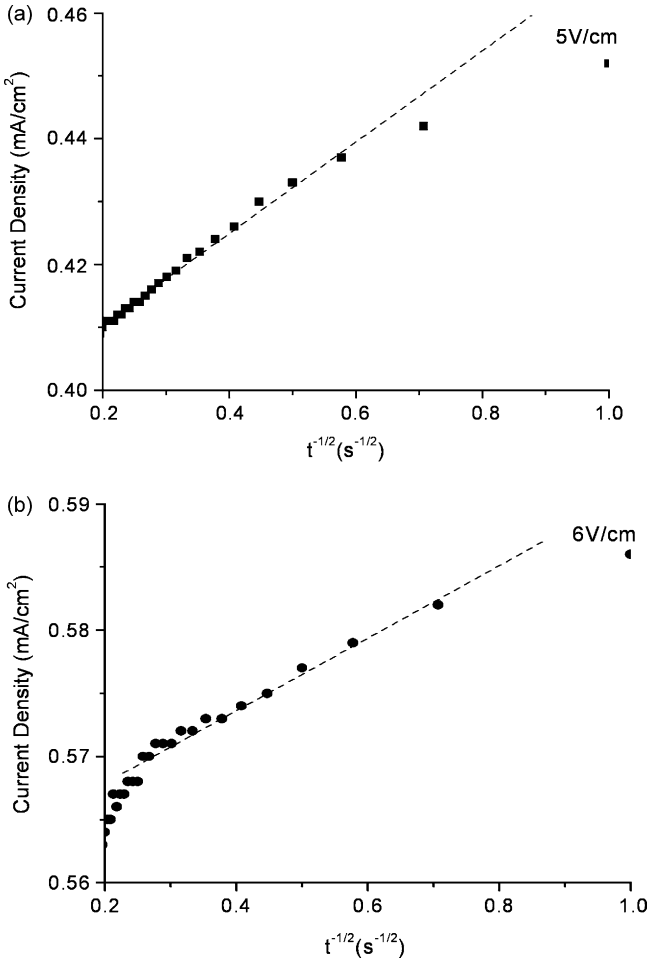

Fig. 4. Currents density vs. inverse square root of deposition duration plot under (a) 5 V/cm and (b) 6 V/cm deposition.

In summary, the moderate electric field of 5–6 V/cm and current density 0.8 mA/cm^2 are reckoned to be the optimum depositions condition for uniform coverage and avoiding poor nanorods adhesion. Oxide layer shielding effect is observed and it could be probably solved by constant current EPD, with further increased deposition voltage, a longer deposition duration and optimum current density.

As reported by Koura et al.,[23] a diffusion controlled process can be described by Cottrell equation:

$$i = \frac{KC}{(\pi Dt)^{1/2}} \quad (2)$$

where i is the current, K is the kinetic constant, D is the diffusion coefficient and t is the deposition duration. The equation can be simplified to $i = kt^{-1/2}$ when K, C and D are kept as constant. Fig. 4a and b show the experimental data of 5 V/cm and 6 V/cm deposition separately. It is observed that both cases follow the Cottrell equation where the i–$t^{-1/2}$ curves shows an almost linear relationship with a similar slope, which suggests the deposition presented in this work is a diffusion controlled process. Deviation from the slope is observed at long deposition time. This deviation could be due to the build-up of the oxide layer which decreases the nanorods electrophoresis in the suspension and the detected current containes significant parasitic currents such as water electrolysis.

3.2. Electrochromic studies

The EPD coated WO_3 nanorods were tested for UV–vis transmittance under a switching voltage of ±3 V (Fig. 5a). The WO_3 nanorods were bleached at +3 V with around 60% of transmittance at 700 nm and exhibited strong absorption of red-end light at −3 V biasing. The transmittance modulation at 700 nm ($\Delta T_{700\,nm}$) is found to be around 40%, which is comparable to other crystalline films.[24,25] Switching time of the WO_3 nanorods is extracted from the transmittance data in Fig. 5b by applying a square wave voltage of ±3 V to the oxide layer (simulating the switching condition). The switching time – bleaching (t_b) and coloring (t_c) time are calculated as the time required for 70% optical modulation in order to compare with literatures. Coloration time $t_c^{70\%}$ is found to be 28.8 s, which is comparable to the reported values ($t_b \sim 25$ s).[26] However, the bleaching time $t_b^{70\%}$ of 4.5 s is found to be much superior than the crystalline[26] ($t_b \sim 22$ s) and amorphous WO_3 ($t_b \sim 18$–36 s).[26,27] This improvement is attributed to the porous nature of the oxide layer which consists of nanorods. The porous

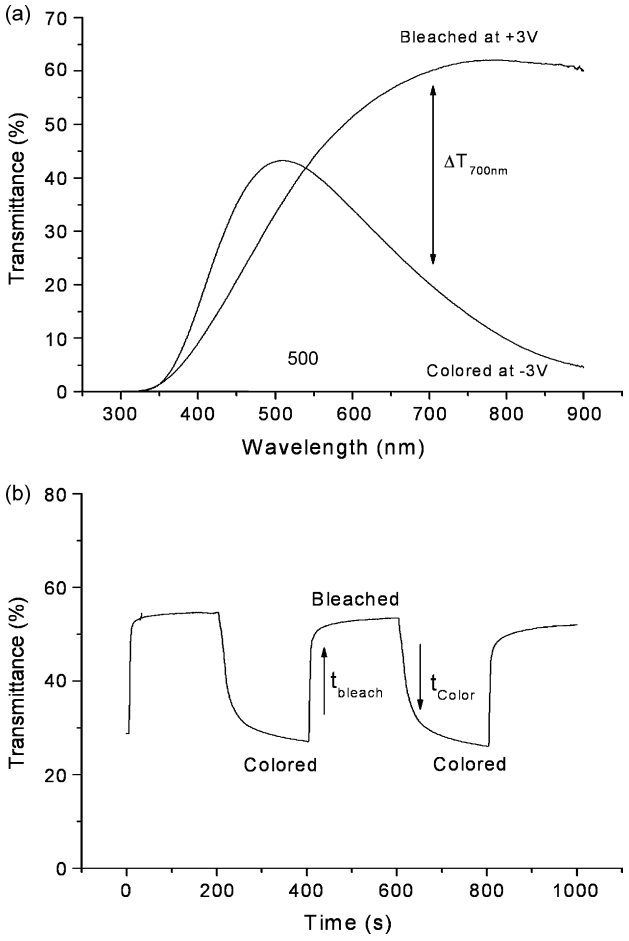

Fig. 5. (a) UV–vis transmittance of WO_3 nanorods at bleaching (+3 V) and coloring (−3 V); (b) switching study by applying a square wave signal ±3 V at 632.8 nm. All electrochemical studies were carried out in 1 M $LiClO_4$/PC electrolyte.

oxide layer allows the electrolyte penetration and hence shortens the ionic diffusion length from the electrolyte to the centre of the oxide. On the other hand, the high surface to volume ratio of the nanorods oxide layer facilitats the Li^+ ion movement across the oxide–electrolyte interface by a providing large amount of reaction sites. Hence, shorter switching time is observed as the result of these two factors.

4. Conclusion

WO_3 nanorods electrophoretic deposition (EPD) has been demonstrated for a thin layer coating ∼1.2 μm for electrochromic application. The optimum EPD conditions were found to be at 0.8 mA/cm^2 or 5–6 V/cm in 10 mg/cm^3 WO_3 nanorods suspension. Oxide layer shielding effect was observed in the constant voltage EPD while the nanorods deposition ceased after 900 s of deposition. Constant current EPD has been performed and the deposited amount was found to be proportional to the charge passed through the electrode. However, oxide layer peel off occured at high current density (>0.8 mA/cm^2) due to the poor adhesion of the nanorods at high deposition rate. The process was shown to be a diffusion controlled process as the i vs. $t^{-1/2}$ plot showed a linear relationship. The EPD coated WO_3 nanorods exhibited a moderate coloration time $t_c^{70\%}$ of 28.8 s and significantly improved bleaching time $t_b^{70\%}$ of 4.5 s. The improvement was due to the porous nanorods layer which facilitated the ion extraction by shortening the ionic diffusion length and the large surface area acted as the reaction sites for ion insertion/extraction.

References

1. Niklasson, G. A. and Granqvist, C. G., Electrochromics for smart windows: thin films of tungsten oxide and nickel oxide, and devices based on these. *J. Mater. Chem.*, 2007, **17**, 127–156.
2. Guérin, J., Aguir, K., Bendahan, M. and Lambert-Mauriat, C., Thermal modeling of a WO_3 ozone sensor response. *Sens. Actuators B*, 2005, **104**, 289–293.
3. Lampert, C. M., Large-area smart glass and integrated photovoltaics. *Sol. Energy Mater. Sol. Cells*, 2003, **76**, 489–499.
4. Zhao, Y., Feng, Z. C. and Liang, Y., Pulsed laser deposition of WO-base film for NO gas sensor application. *Sens. Actuators B*, 2000, **66**, 171–173.
5. Granqvist, C. G., Electrochromic tungsten oxide films: review of progress 1993–1998. *Sol. Energy Mater. Sol. Cells*, 2000, **60**, 201–262.
6. Yoo, S. J., Lim, J. W., Sung, Y.-E., Jung, Y. H., Choi, H. G. and Kim, D. K., Fast switchable electrochromic properties of tungsten oxide nanowire bundles. *Appl. Phys. Lett.*, 2007, **90**, 173126.
7. Deepa, M., Srivastava, A. K., Sood, K. N. and Agnihotry, S. A., Nanostructured mesoporous tungsten oxide films with fast kinetics for electrochromic smart windows. *Nanotechnology*, 2006, **17**, 2625–2630.
8. Gu, Z., Li, H., Zhai, T., Yang, W., Xia, Y., Ma, Y. *et al.*, Large-scale synthesis of single-crystal hexagonal tungsten trioxide nanowires and electrochemical lithium intercalation into the nanocrystals. *J. Solid State Chem.*, 2007, **180**, 98–105.
9. Liao, C.-C., Chen, F.-R. and Kai, J.-J., Electrochromic properties of nanocomposite WO_3 films. *Sol. Energy Mater. Sol. Cells*, 2007, **91**, 1258–1266.
10. Subrahmanyam, A. and Karuppasamy, A., Optical and electrochromic properties of oxygen sputtered tungsten oxide (WO_3) thin films. *Sol. Energy Mater. Sol. Cells*, 2007, **91**, 266–274.
11. Lee, S.-H., Deshpande, R., Parilla, P. A., Jones, K. M., To, B., Mahan, A. H. *et al.*, Crystalline WO_3 nanoparticles for highly improved electrochromic applications. *Adv. Mater.*, 2006, **18**, 763–766.
12. Van der Biest, O. O. and Vandeperre, L. J., Electrophoretic deposition of materials. *Annu. Rev. Mater. Sci.*, 1999, **29**, 327–352.
13. Sarkar, P. and Nicholson, P. S., Electrophoretic deposition (EPD): mechanisms, kinetics, and application to ceramics. *J. Am. Ceram. Soc.*, 1996, **79**, 1987–2002.
14. Boccaccini, A. R. and Zhitomirsky, I., Application of electrophoretic and electrolytic deposition techniques in ceramics processing. *Curr. Opin. Solid State Mater. Sci.*, 2002, **6**, 251–260.
15. Girishkumar, G., Vinodgopal, K. and Kamat, P. V., Carbon nanostructures in portable fuel cells: single-walled carbon nanotube electrodes for methanol oxidation and oxygen reduction. *J. Phys. Chem. B*, 2004, **108**, 19960–19966.
16. Boccaccini, A. R., Cho, J., Roether, J. A., Thomas, B. J. C., Minay, E. J. and Shaffer, M. S. P., Electrophoretic deposition of carbon nanotubes. *Carbon*, 2006, **44**, 3149–3160.
17. Yu, J. and Zhou, M., Effects of calcination temperature on microstructures and photocatalytic activity of titanate nanotube films prepared by an EPD method. *Nanotechnology*, 2008, **19**, 1–6.
18. Wang, J., Khoo, E., Lee, P. S. and Ma, J., Synthesis, assembly, and electrochromic properties of uniform crystalline WO_3 nanorods. *J. Phys. Chem. C*, 2008, **112**, 14306–14312.
19. Kuwabara, K. and Noda, Y., Electrophoretic preparation of antimonic acid film. *J. Mater. Sci.*, 1993, **28**, 5257–5261.

20. Ma, J. and Cheng, W., Deposition and packing study of sub-micron PZT ceramics using electrophoretic deposition. *Mater. Lett.*, 2002, **56**, 721–727.
21. Jung, S. M., Jung, H. Y. and Suh, J. S., Horizontally aligned carbon nanotube field emitters fabricated on ITO glass substrates. *Carbon*, 2008, **46**, 1973–1977.
22. Yui, T., Mori, Y., Tsuchino, T., Itoh, T., Hattori, T., Fukushima, Y. *et al.*, Synthesis of photofunctional titania nanosheets by electrophoretic deposition. *Chem. Mater.*, 2005, **17**, 206–211.
23. Koura, N., Tsukamoto, T., Shoji, H. and Hotta, T., Preparation of various oxide films by an electrophoretic deposition method: a study of the mechanism. *Jpn. J. Appl. Phys.*, 1995, **34**, 1643–1647.
24. Liao, C.-C., Chen, F.-R. and Kai, J.-J., WO_{3-x} nanowires based electrochromic devices. *Sol. Energy Mater. Sol. Cells*, 2006, **90**, 1147–1155.
25. Joraid, A. A., Comparison of electrochromic amorphous and crystalline electron beam deposited WO_3 thin films. *Curr. Appl. Phys.*, 2009, **9**, 73–79.
26. Sallard, S., Brezesinski, T. and Smarsly, B. M., Electrochromic stability of WO_3 thin films with nanometer-scale periodicity and varying degrees of crystallinity. *J. Phys. Chem. C*, 2007, **111**, 7200–7206.
27. Deepa, M., Singh, D. P., Shivaprasad, S. M. and Agnihotry, S. A., A comparison of electrochromic properties of sol–gel derived amorphous and nanocrystalline tungsten oxide films. *Curr. Appl. Phys.*, 2007, **7**, 220–229.